Effect of RF Pulse Repetition Time on Gas Transfer for Dissolved Hyperpolarized ^{129}Xe MRI

Brandon Zanette[1,2], Matthew S Fox[3], Ozkan Doganay[3,4], Elaine Hegarty[2,3], and Giles E Santyr[1,2]

[1]*Department of Medical Biophysics, University of Toronto, Toronto, Ontario, Canada,* [2]*Peter Gilgan Centre for Research and Learning, The Hospital for Sick Children, Toronto, Ontario, Canada,* [3]*Robarts Research Institute, London, Ontario, Canada,* [4]*Department of Medical Biophysics, University of Western Ontario, London, Ontario, Canada*

Introduction: MRI following inhalation of hyperpolarized ^{129}Xe gas promises to provide unique anatomical and functional information for diagnosis of pulmonary disease. In particular, ^{129}Xe readily dissolves in the tissue and blood compartments of the lung allowing for quantification of regional gas exchange, taking advantage of the large chemical shift differences between gaseous and dissolved ^{129}Xe in the tissue and red blood cell (RBC) compartments respectively[1]. However, the dissolved phases represent only about 2% of the xenon concentration in the lung, and accumulation of sufficient tissue and RBC ^{129}Xe signal is a significant challenge. Performing multiple acquisitions of the dissolved ^{129}Xe spectra using high flip angle (eg. 90°) frequency-selective RF pulses that avoid depolarization of the gas phase is a solution[2]. Similar to conventional Saturation Recovery in proton MRI, dissolved phase ^{129}Xe SNR may be increased by allowing "recovery" (ie. replenishment) of dissolved signal from the gas phase reservoir in a repetition time between pulses (TR) sufficiently long compared to the compartmental gas transfer time (T_{TR}). A further constraint is that TR must be short enough to provide a total imaging time that does not exceed a reasonable breath-hold interval (e.g. 15s). In this work we investigate the optimization of TR for various breath-hold imaging strategies using an established gas exchange model described in Mansson et al.[3] and ^{129}Xe Chemical Shift Saturation Recovery (CSSR)[4] signal versus time curves characterizing uptake for both tissue and RBC compartments. The model is extended to the specific application of distinguishing tissue and RBC gas exchange abnormalities associated with radiation-induced lung injury (RILI) in a rat model.

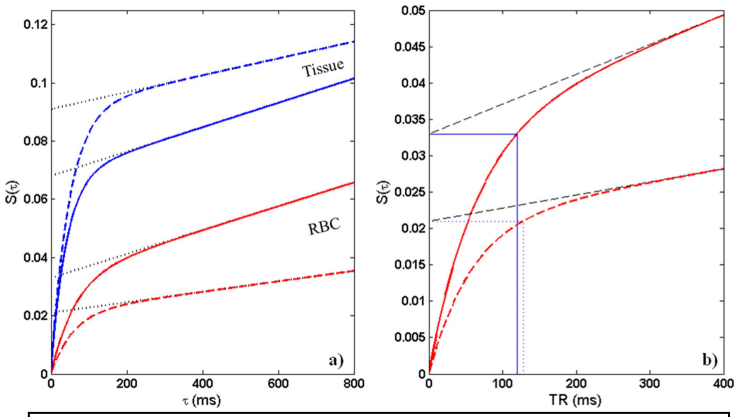

Fig.1a) Average fitted CSSR curves for tissue and RBC compartments as a function of delay time. **b)** RBC signal curves as a function of TR. Solid and dashed curves represent healthy and irradiated cohort, respectively.

Methods: ^{129}Xe CSSR curves for tissue and RBC compartments consisting of 14 delay times (τ) ranging from 0.76ms to 3001ms, were obtained for cohorts of healthy (n=6) and irradiated (n=5) rats as described previously by Fox et al.[5]. A three-parameter xenon gas transfer model[3] of the form

$$S(\tau)=S_0(1-\exp(-\tau/T_{TR}))+S_1\tau \quad [1]$$

was fit to the CSSR signals to extract average fit parameter estimates for tissue and RBC compartments for the two cohorts. These estimates were then used to simulate representative ^{129}Xe tissue and RBC signal uptake curves as a function of TR for control and RILI rats. Optimal TR was determined when the weaker of the two signals (determined by S_0) reaches S_0. At this point the linear portion of curve (black dashed lines, Fig.1) outpaces the exponential term in Eqn. [1]. Increases in TR beyond this point result in diminishing signal returns and may result in unacceptably long breath-hold times (>15s). The compartment with lower S_0 (i.e. RBC) was chosen as a threshold for determining the optimal TR because it is the rate-limiting step; the other compartment (i.e. tissue) will inherently have more accumulation at the same time.

Results: Average fitted parameters extracted from individual CSSR curves for both cohorts are shown in Table 1. Figure 1a shows the average fitted CSSR curves for both tissue and RBC compartments for both cohorts. Figure 1b shows simulated RBC signal as a function of TR for both cohorts. The optimal TR values to discriminate RBC and tissue changes induced by irradiation were determined to be 120ms (control) and 128ms (RILI) as shown by the solid and dashed vertical lines, respectively, while the horizontal lines mark S_0.

Discussion: Although the non-renewable nature of hyperpolarized ^{129}Xe would indicate the shortest possible TR for efficient gas phase imaging is desirable, this work emphasizes this is not the case for the dissolved phases where considerable improvement in signal is possible at longer TR values due to gas transfer. This is dependent on the specific xenon gas transfer properties of lung tissue and RBC compartments as characterized by the CSSR curves. For the RILI application investigated here, the CSSR curves (Fig.1) continue to increase as a function of time. This means that for purely spectroscopic (i.e. single voxel applications) increases in TR lead to SNR improvements, provided the acquisition is completed within an acceptable breath-hold interval. As spectral information is traded for spatial resolution, efficient use of the replenishment of dissolved ^{129}Xe compartments via the gas phase is increasingly sensitive to TR. Fig.1 shows that spectroscopic imaging pulse sequences (e.g. Dixon based) requiring shorter TR values (10-100ms) to perform efficient spatial encoding of the dissolved phases within a breath-hold may lead to incomplete replenishment of signal, resulting in decreased SNR. Therefore it may be advantageous to consider alternate spatial encoding strategies (sectoral, spiral) that permits increases in TR without sacrificing spatial resolution for improvement in dissolved phase ^{129}Xe SNR within a breath-hold. Such approaches also make more efficient use of the non-renewable hyperpolarized magnetization by using fewer RF pulses with higher flip angles. It was observed that even though uptake in the irradiated rats was attenuated by RILI, choice of optimal TR determined from $S(\tau)=S_0$ did not differ greatly between cohorts (TR=120-130ms), thereby not affecting discrimination of injured from healthy tissue. The results of this work have applications in human imaging, where timing is of greater consequence and in other disease models where signal uptake may be further attenuated than observed in this case, requiring longer delay times and additional temporal constraints. Characterization of other diseases using CSSR is required in order to estimate compartmental replenishment.

	Control		RILI	
Parameter	**Tissue**	**RBC**	**Tissue**	**RBC**
S_0	0.068±0.014	0.033±0.005	0.091±0.015	0.021±0.005
T_{TR} (ms)	39.76±10.32	62.82±33.31	47.63±8.05	57.91±20.91
$S_1(\times 10^{-5}\,ms^{-1})$	4.19±2.33	4.10±1.39	2.90±1.24	1.80±1.05

Table 1: Average gas transfer parameters extracted from the 3-parameter curve fit to CSSR curves (Fig.1a) for healthy (n=6) and irradiated (n=5) rat cohorts.

Acknowledgements: Funding support for this work from NSERC, CIHR, and The Hospital for Sick Children is gratefully acknowledged.

References: 1. Sakai et al., J Magn. Reson. B. (1996), 111:300-304. 2. Kaushik et al., J. Appl. Physiol. (2014), 117:577-585. 3. Ruppert et al., NMR Biomed. (2000), 13:220-228. 4. Mansson et al., MRM (2003), 50:1170-1179. 5. Fox et al., Med. Phys. (2014), 41.